International Journal of Automotive Technology, Vol. 23, No. 5, pp. 1393–1403 (2022)
DOI 10.1007/s12239–022–0122–y

pISSN 1229–9138/ eISSN 1976–3832

ADAPTIVE ENERGY MANAGEMENT STRATEGY OF FUEL CELL ELECTRIC VEHICLE

Yan Sun[1)], Changgao Xia[1)], Bifeng Yin[1)], Yingxiao Yu[1)*], Jiangyi Han[1)] and Haiyu Gao[2)]

[1)]School of Automotive and Traffic Engineering, Jiangsu University, Zhenjiang 212013, China
[2)]Fuel Cell Vehicle Technology Research Center, D. R. Power Technology Co., Ltd., Room 2401, Block B, No.705, Yatai Road, Nanhu District, Jiaxing, Zhejiang 314000, China

(Received 23 September 2021; Revised 7 January 2022; Accepted 30 March 2022)

ABSTRACT–The energy management strategy (EMS) can efficiently split the power among different sources for a fuel cell electric vehicle (FCEV). This paper puts forward how to cooperate with a proton exchange membrane fuel cell as the primary energy source, and a ultracapacitor as the auxiliary energy storage. Firstly, the test bench of fuel cell is built and the characteristic of fuel cell is tested. A model of vehicle is built in AMESim software based on the real parameters of vehicle especially the characteristic of fuel cell. Secondly, the traditional power following strategy is introduced and an optimal energy management strategy is proposed. The demand power is decomposed by quadratic utility function (QUF) and Karush-Kuhn-Tucker (KKT) condition. In order to balance the vehicle economy and durability of fuel cell, the multi-objective artificial bee colony algorithm (MOABC) and pareto solution set are used to solve the optimal balance coefficient in the algorithm. The simulation results show that compared with the traditional strategy under one WLTP driving cycle, the novel strategy can reduce the fuel cell degradation by 25.08 %, and the equivalent hydrogen consumption can be also reduced.

KEY WORDS : Energy management strategy, KKT condition, Quadratic utility function, Durability of fuel cell

1. INTRODUCTION

In order to reduce the emissions of vehicles, the electric vehicles (EVs) are proposed. However, limited driving range and slow charging problems cannot be fundamentally solved so far (Yu and Ahn, 2019; Hu *et al*., 2021; Gharibeh *et al*., 2020). The plug-in hybrid electric vehicles (PHEVs) which are powered by internal combustion engines (ICE) can effectively solve the problems. However, ICE still have a considerable amount of pollutant emissions (Mebarki *et al*., 2015; Bin *et al*., 2020). Fuel cell electric vehicle (FCEV) is developed as an effective solution (Zhou *et al*., 2020; Hwang *et al*., 2015; Karaoğlan *et al*., 2019). A good durability can be ensured for the FCEV when slow load dynamics are applied in practice (Erdinc and Uzunoglu, 2010). An energetic buffer such as battery and ultracapacitor should be used with the proton exchange membrane fuel cell (PEMFC) to satisfy the fast dynamic load (Rajabzadeh *et al*., 2016). Therefore, the energy management strategy of multi power sources has become the core problem affecting the economy and durability of the vehicle. Compared with batteries, ultracapacitors have lower mass, lower cost, longer life and faster output dynamic response, which is considered to be the best combination with fuel cells.

Previous studies have shown that energy management strategies (EMSs) are mainly divided into three classes: rule-based strategies, optimization-based strategies and intelligent-based strategies (Sulaiman *et al*., 2018). The rule-based (RB) strategy includes deterministic rules and fuzzy rules. Wang *et al*. (2019) proposed a rule-based strategy, in which the case conditions of different operation modes were discussed. The hydrogen consumptions of 10 %, 30 %, and 50 % SOC thresholds were 1.15 kg, 1.27 kg and 1.38 kg. Regarding fuzzy rules, Li *et al*. (2020) used fuzzy control method to optimize the output power of the fuel cell. The rules are made in advance to control the output power of each power sources. The algorithm is simple and easy to be applied, but the rule formulation is mostly based on the experience of experts, so it is impossible to achieve optimal goal and cannot meet the needs of changeable road conditions and dynamic changes.

The optimization-based methods are mainly divided into global optimization and real-time optimization. Dynamic programming (DP), linear programming (LP), particle swarm optimization (PSO), genetic algorithm (GA), extremum seeking (ES), and so on are usually used for global optimization. Pontryagin's minimum principle (PMP), equivalent consumption minimization strategy (ECMS), model predictive control (MPC), convex

**Corresponding author*. e-mail: yyx@ujs.edu.cn

programming (CP) and so on are usually used for real-time optimization (Sorlei *et al*., 2021). Dynamic programming is a typical example of global optimization. Zhou *et al*. (2018) proposed a unified dynamic programming model, which improved the calculation accuracy and efficiency of FCEV. MPC transforms the optimal fuel economic performance control of the whole road section into the local fuel economic performance optimal control in the predicted area, and it has the advantages of convenient modeling, high robustness and good dynamic control performance (Chen *et al*., 2013).

In recent years, artificial intelligence has developed rapidly (Xie *et al*., 2020; Mbuwir *et al*., 2021). Lian *et al*. (2020) investigated a rule-interposing deep reinforcement learning (RIDRL) based energy management strategy (EMS) of hybrid electric vehicle (HEV). By allocating weights between the fuel consumption and the battery charge sustaining properly, fuel consumption was significantly reduced by up to 4 %. The simplified action space improves the convergence efficiency by 70.6 %. Qi *et al*. (2019) designed a deep reinforcement learning based real-time energy management system. The proposed model combined a Q-learning and a deep neural network to form a deep Q-network structure which was capable of learning and providing the optimal control decisions in continuous environment and actions states.

Fuel economy is an important optimization goal of EMS. Based on the Charge-Depleting/Charge-Sustaining (CDCS) strategy, Chen *et al*. (2015) used the particle swarm optimization (PSO) to optimize the output power of extender. The lowest energy consumption was realized in the Charge Sustaining (CS) mode. Fernández *et al*. (2018) used GA to optimize the output current and turn-on time of fuel cell. The hydrogen consumption was minimized and the SOC of battery was maintained at a low level. Based on PMP, Ouddah *et al*. (2018) combined the system's S function with the formula of the control objective, the optimal value of the control variable was determined at each time. So as to minimize the power consumption of the hybrid electric bus, Zheng *et al*. (2012) found the fuel-saving potential of ECMS was around 4 % relative to RB, but it may lead to frequent fluctuations in fuel cell output power, which accelerated the degradation of fuel cell. Based on the maximum power point tracking algorithm, Bizon and Thounthong (2018) took the fuel economy as the optimization goal, the results showed that the global optimization has great advantages in improving the economy.

Fuel cells have a short lifespan, and the degradation of fuel cell is affected by many factors, such as load changing cycles, start-stop cycles, idling and high-power load conditions, etc. These factors will reduce the cycle life of fuel cell (Borup *et al*., 2020). Start-stop cycles are the main factor affecting the degradation of fuel cell. Zhang *et al*. (2018) pointed out that start-stop cycles account for about 33 % of the whole degradation of fuel cell. Zhang *et al*. (2019) proposed a strategy based on three fuel cell stack systems to reduce the start-stop cycling of fuel cells. The results showed that this method could decrease the start-stop cycles of fuel cell under various combined cycle conditions, and the average start-stop cycling is 15.2 times per hour, which is considered acceptable. Sun *et al*. (2020) decreased degradation losses of fuel cell based on min-max game theory, in which the start-stop cycling is about 4.2 times per hour. It can be seen that, the lower the start-stop frequency is, the better the durability is. But too much consideration of durability will lead to the decrease of economy (Liu *et al*., 2020).

Although the current EMS can reduce energy consumption, extend the driving range, and increase the lifespan of power sources, the input and output characteristics of power sources are seldom considered. When the demand current rises suddenly, the response of the fuel cell is slow. If the established EMS is followed, it will cause a large deviation between the demand power and the actual power, which will affect the vehicle's power performance and economy.

In this paper, a novel adaptive EMS for FCEV is proposed and it considers the hydrogen consumption, lifespan of fuel cell. The information of the current and history states of the vehicle is also considered in the strategy. The proposed strategy is an optimal online strategy with the idea of offline optimization. The change rate of the fuel cell current is taken into consideration as a key constraint, which is ignored by others. The rest of this paper is arranged as follows: in Section 2, the model of the FCHV is presented, the fuel cell and ultracapacitor simulation models are built. The fuel cell test bench is also designed to make the test conditions consistent with the driving conditions. Section 3 describes the traditional power following strategy. Section 4 describes the novel EMS, the required power is decomposed into the target power of fuel cell and ultracapacitor by partial differentiation of quadratic utility function and combined with Karush-Kuhn-Tucker condition. In section 5, the multi-objective artificial bee colony algorithm and pareto solution set are used to solve the optimal balance coefficient in the algorithm. In Section 6, the case study is described and the results obtained by simulations are shown. Finally, the conclusions and a prospective are drawn in section 7.

2. SYSTEM MODEL

2.1. System Description

In this paper, a representative powertrain structure with a fuel cell/ultracapacitor hybrid system is used to discuss the EMS of a FCEV. Figure 1 presents the system structure, the system structure includes a fuel cell stack, DC/DC, ultracapacitor, E-machine, air compressor, intercooler, humidifier, water pump, hydrogen circulating pump, hydrogen container and so on. The DC/DC includes a

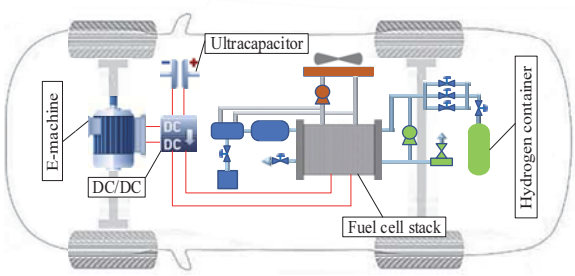

Figure 1. System structure.

unidirectional boost converter and a bidirectional buck/boost converter. The unidirectional boost converter connects PEMFC to DC-bus. The bidirectional buck/boost converter connects ultracapacitor to DC-bus. The e-machine provides power to the vehicle and converts the braking energy into electrical energy.

2.2. Ultracapacitor Model

The use of ultracapacitors in the hybrid electric vehicle is very important. Due to the irreversible energy conversion of fuel cell, the braking energy of vehicle is mainly recovered by ultracapacitor. The ultracapacitor model consists of capacitor C, equivalent series resistance R_{uc} and leakage resistance R_L. The ultracapacitor model is derived as follows:

$$\begin{cases} V_{uc} = V_{ocv} - I_{uc} \cdot R_{uc} \\ P_{uc} = V_{uc} \cdot I_{uc} \\ \dfrac{dV_{tem}}{dt} = -\dfrac{I_{uc} + I_L}{C} \\ I_L = U_{tem} / R_L \\ V_{tem} = \left[V_{C0} \displaystyle\int_0^t \frac{I_{uc}}{C} e^{t/(C \cdot R_L)} dt \right] e^{-t/(C \cdot R_L)} \end{cases} \quad (1)$$

where V_{tem} is the terminal voltage of ultracapacitor, V_{uc} is the output voltage, P_{uc} is output power, I_{uc} is the output current, I_L is the leakage current, V_{C0} is the initial voltage, and SOC is the state charge of ultracapacitor.

2.3. PEMFC System

This paper establishes a static model of a PEMFC system, the ambient temperature, humidity, and gas pressure of fuel cell system are all in steady state. The relationship between output power and efficiency of fuel cell system is showed in Figure 2. Fuel cell is less efficient when operating in low power mode, because the fuel cell stack assist system consumes most of the power. Whereas the efficiency is also reduced in high load power mode due to physical restrictions of the fuel cell stack. To include a parasitic load

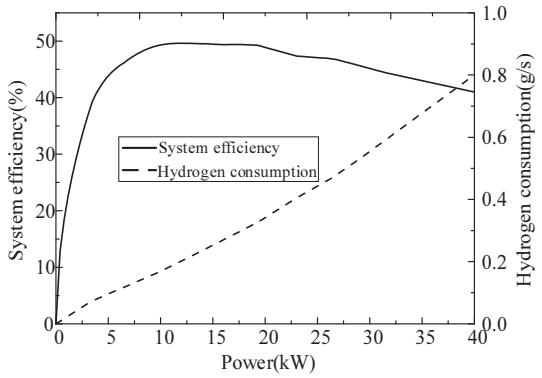

Figure 2. Fuel cell system efficiency and hydrogen consumption rate.

for cooling and air supply, a static power consumption is considered. The hydrogen consumption can be calculated by Equation (2). The working efficiency of fuel cell system η_{fc} can be expressed in terms of fuel cell's net output power P_{fc}.

$$\begin{cases} P_{fc}(t) = N_{fc} \cdot P_{fc\text{-}stack}(t) - P_{BOP}(t) \\ M_{H2} = \dfrac{1}{J_{low}} \displaystyle\int_0^t \frac{P_{fc}(t)}{\eta_{fc}(t)} dt \\ \eta_{fc} = \varphi(P_{fc}) \end{cases} \quad (2)$$

where $P_{fc}(t)$ is the net output power of fuel cell system, $P_{BOP}(t)$ is the power consumed by all BOP (Balance of Plant), N_{fc} is the number of the active fuel cell stacks at a certain instant time, $P_{fc\text{-}stack}$ is the output power of each fuel cell stack, M_{H2} is the hydrogen consumption of fuel cell system, J_{low} is the low heating value of hydrogen, and $\eta_{fc}(t)$ is the working efficiency of fuel cell system.

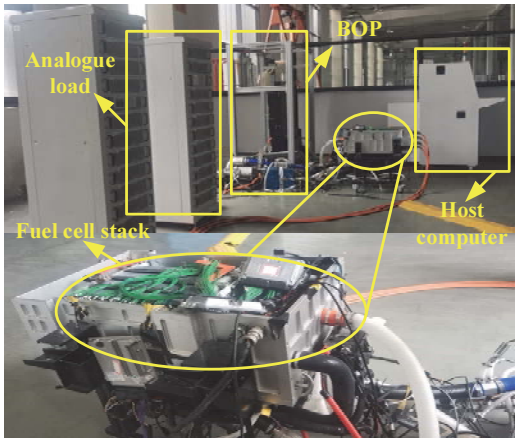

Figure 3. Fuel cell system test bench.

The required data of fuel cell model in this paper comes from the real bench test. The test bench includes analogue load, fuel cell stack, BOP and so on. The BOP includes cooling system, air filter, air compressor and so on. The test bench is shown in Figure 3.

2.4. Lifespan Model

The performance degradation of fuel cell is the key factor to be considered. In this section, a lifespan model of fuel cell is established, which mainly includes four parts: load changing cycles, start-stop cycles, idling and high-power load conditions, as shown in Equation (3):

$$D_{fc}^{*}=D_{change}+D_{on\text{-}off}+D_{idl}+D_{high} \tag{3}$$

where D_{fc}^{*} is the total performance degradation of fuel cell. D_{change}, $D_{on\text{-}off}$, D_{idl}, D_{high} are performance degradation caused by load changing cycles, start-stop cycles, idling/low power conditions, and high-power load conditions.

In order to improve the efficiency of the fuel cell system, the output power of fuel cell system is limited within its high efficiency region. Therefore, the performance degradation caused by idling and high-power load conditions can be ignored in the total degradation of fuel cell mentioned above. The actual fuel cell degradation model is as follows (Song *et al*., 2018):

$$D_{fc}=D_{change}+D_{on\text{-}off} \tag{4}$$

$$\begin{cases} D_{change}=5.93\times10^{-7}\times\sum\dfrac{|P_{fc}(n)-P_{fc}(n-1)|}{P_{high}-P_{low}} \\ D_{on\text{-}off}=1.96\times10^{-5}\times\sum d_{on\text{-}off}(n) \\ d_{on\text{-}off}(n)=1, \quad signal_{fc}(n-1)\neq signal_{fc}(n) \\ d_{on\text{-}off}(n)=0, \quad signal_{fc}(n-1)=signal_{fc}(n) \end{cases} \tag{5}$$

where D_{fc} is the actual equivalent performance degradation of fuel cell in this paper, P_{low} is the low-power threshold of the fuel cell under idling conditions, P_{high} is the high-power threshold. $signal_{fc}(n)$, and $signal_{fc}(n\text{-}1)$ are fuel cell system start signal of the n step and n-1 step ('0' indicates shutdown, '1'indicates normal operation).

2.5. Powertrain Model

The required power P_{dem} is calculated as a function of driving force and speed, as shown in Equation (6).

$$\begin{aligned} P_{dem}=&M_{vel}\cdot g\cdot V(t)\{C_r\cos(\theta)+\sin(\theta)\}+ \\ &M_{equ}\cdot\frac{dV(t)}{dt}\cdot V(t)+0.5C_d\cdot A\cdot\rho\cdot V^3(t) \end{aligned} \tag{6}$$

where M_{vel} is the total mass of vehicle, $V(t)$ is the speed of vehicle, C_r is the coefficient of rolling resistance, θ is the slope angle of the ramp, M_{equ} equals $1.2\cdot M_{vel}$ to suitably account for rotational inertia, C_d is the coefficient of air resistance, A is the windward area, and ρ is the air density.

3. TRADITIONAL POWER FOLLOWING STRATEGY

The traditional power following strategy is a typical control strategy, which has been widely studied. The traditional power following strategy is simple and practical, and which is widely used in practical FCEVs. In the traditional power following control strategy, the control method for the output power of the fuel cell is based on the power required of the vehicle and adjusted by the equilibrium power obtained by taking SOC value as the independent variable. The minimum limit of SOC is set to SOC_{min} = 10, if the ultracapacitor SOC is less than 10 %, the fuel cells provide the maximum power. The maximum limit of SOC is set to SOC_{max} = 90, if the SOC of the ultracapacitor is higher than 90 % and the demand power is not very large, the fuel cell does not start to work. When $SOC_{min} < SOC < SOC_{max}$, the control objective is based on satisfying dynamic performance, the ultracapacitor provides output power to reduce outpower of fuel cell and increase the driving mileage. The required power algorithm for the FCEV can be expressed as follows (Geng *et al*., 2019):

$$\begin{cases} P_{fc}=P_{fcmax} \quad , \quad P_{dem}>P_{mot\_max} \\ P_{fc}=\gamma\left(\dfrac{SOC_{max}-SOC}{SOC_{max}-SOC_{min}}\right)\bullet \\ \qquad \dfrac{P_{dem}}{P_{mot\_max}}\bullet P_{fc\max} \quad , \quad P_{dem}\le P_{mot\_max} \\ P_{uc}=P_{dem}-P_{fc} \end{cases} \tag{7}$$

where P_{mot_max} is the maximum motor power in the maximum efficiency range of the motor, and γ is the adjustment coefficient.

The traditional power following strategy only considers problem of the SOC maintenance of ultracapacitors and energy distribution, but ignores the fuel cell life protection and vehicle economy.

4. NOVEL EMS DESIGN

4.1. Strategy Analysis

The EMS is developed to increase the fuel cell lifespan, maintain the ultracapacitor SOC, and increase driving range. The ultracapacitor has a high power density and it can be used to absorb and release large current quickly, thus the fluctuation of fuel cell output power can be reduced.

In this section, a quadratic utility function is used to quantify the benefits of fuel cells and ultracapacitors in energy distribution. Quadratic utility function forms are as follows (Ma *et al*., 2016):

$$U=1-\lambda_1 x-\lambda_2 x^2 \tag{8}$$

where U is the utility function, x is the variable, and λ_1, λ_2 are the coefficients.

4.2. Utility Function of Fuel Cell

For the fuel cell, durability and economy are the main consideration, i.e. reducing the load changing cycles, start-stop cycles of the fuel cell and maintaining the fuel cell efficiency at the top efficiency point. The utility function of the fuel cell is equivalent to the utility of the fuel cell's lifespan and efficiency in this paper, which contains two parts, U_{fc_dua} and U_{fc_eco}. The aim of U_{fc_dua} is to minimize the minimize the power variation (dP_{fc}/dt) of the fuel cell while the aim of U_{fc_eco} is to maximize the efficiency of fuel cell, as shown in Equation (9).

$$\begin{cases} U_{fc} = k_{dua}\ U_{fc\_dua} + k_{eco}\ U_{fc\_eco} \\ U_{fc\_dua} = 1-a_1\ (P_{fc}-P_{fc,l})^2 \\ U_{fc\_eco} = 1-a_2\ (P_{fc}-P_{fc,top})^2 \end{cases} \tag{9}$$

where k_{dua}, and k_{eco} are the weight coefficients, $P_{fc,l}$ is the output power of the fuel cell at last one second, which is used to obtain dP_{fc}/dt, and $P_{fc,top}$ is the output power of fuel cell at the top efficiency point.

The coefficient a_1 is used to normalize the value of U_{fc_dua} to be zero when dP_{fc}/dt comes to its maximum threshold, as shown in Equation (10). Since the maximum value of dP_{fc}/dt determines the maximum power variation that the system could take, bench test results show that the maximum change of fuel cell power is 5 kW/s. The coefficient a_2 can be calculated using Equation (11), which is designed to normalize the value of U_{fc_eco} to be zero when P_{fc} comes to its maximum value P_{fcmax}.

$$a_1 = \frac{1}{[\max(P_{fc}-P_{fc,l})]^2} \tag{10}$$

$$a_2 = \frac{1}{(P_{fcmax}-P_{fc,top})^2} \tag{11}$$

4.3. Utility Function of Ultracapacitor

For ultracapacitor, the effect of frequent charging and discharging on its lifespan is not needed to be considered, because the lifespan of ultracapacitor is more than 5 years. Only the maintenance of ultracapacitor *SOC* is needed to be considered. The utility function of ultracapacitor is shown as follows:

$$\begin{cases} U_{uc} = k_{sus}\ U_{sus} \\ U_{sus} = 1-a_3\ (P_{uc}-P_{uc,fit})^2 \\ P_{uc,fit} = (2\dfrac{SOC_{max}-SOC}{SOC_{max}-SOC_{min}}-1)\ P_{ucmax} \end{cases} \tag{12}$$

$$a_3 = \frac{1}{(P_{ucmax}-P_{uc,fit})^2} \tag{13}$$

where U_{uc} is the utility function of ultracapacitor, $P_{uc,fit}$ and P_{ucmax} are the optimal output power and maximum output power of the ultracapacitor respectively, and k_{sus} is the weight coefficient.

In addition, fuel cell and ultracapacitor need to meet the following constraints:

$$\begin{cases} k_{dua}+k_{eco}+k_{sus}=1 \\ 1\geq(k_{dua},k_{eco},k_{sus})\geq 0 \\ P_{fc}+P_{uc}=P_{dem} \end{cases} \tag{14}$$

4.4. KKT Condition

Due to the simplicity of the problem in Equation (14), Karush-Kuhn-Tucker (KKT) conditions is usually used to solve optimization problems with equality and inequality constraints, the optimal objective function is shown in Equation (15). KKT condition is a necessary condition for optimal solution of nonlinear programming. KKT condition extends the constraint optimization problem of Lagrange multipliers involving equality to inequality.

$$\begin{cases} \max f(P_{fc}) = k_{dua}\ U_{fc\_dua} + k_{eco}\ U_{fc\_eco} \\ \max f(P_{uc}) = k_{sus}\ U_{sus} \end{cases} \tag{15}$$

To transform this bi-objective optimization problem into

a single-objective optimization problem, the weighted-sum approach is used. The entire objective function can be formulated as in Equation (16).

$$\min f(P_{fc},\ P_{uc}) = -k_{dua}\ U_{fc\_dua} - k_{eco}\ U_{fc\_eco} - k_{sus}\ U_{sus} \tag{16}$$

Since the inequality constraint in Equation (14) is loose and it can be determined that the optimal solution is not on the boundary of the inequality constraint. The Lagrange Multiplier is used to combine the equality constraint and the objective function into a new function, and the final form is shown as follows:

$$L(P_{fc}, P_{uc}) = -k_{dua}\ U_{fc\_dua} - k_{eco} U_{fc\_eco} - k_{sus}\ U_{sus} + h\ (P_{fc} + P_{uc} - P_{dem}) \tag{17}$$

Let:

$$\frac{\partial L}{\partial P_{fc}} = 2a_1\ k_{dua}\ \ (P_{fc} - P_{fc,l})\ + 2a_2\ k_{eco}\ (P_{fc} - P_{fc,top}) + h = 0 \tag{18}$$

$$\frac{\partial L}{\partial P_{uc}} = 2a_3\ k_{sus}(P_{uc} - P_{uc,fit})\ + h = 0 \tag{19}$$

$$\frac{\partial L}{\partial h} = P_{fc} + P_{uc} - P_{dem} = 0 \tag{20}$$

The extremum can be obtained by solving Equations (18) ~ (20) simultaneously:

$$P_{fc}^{*} = \frac{a_1\ k_{dua}\ P_{fc,l} + a_2\ k_{eco}\ P_{fc,top} + a_3\ k_{sus}\ (P_{dem} - P_{uc,fit})}{a_1\ k_{dua} + a_2\ k_{eco} + a_3\ k_{sus}} \tag{21}$$

$$P_{uc}^{*} = P_{dem} - P_{fc} \tag{22}$$

The Hessian matrix of Equation (17) is:

$$\nabla^2 L = \begin{bmatrix} 2a_1\ W_{dua} & 0 \\ 0 & 2a_3\ W_{sus} \end{bmatrix} \tag{23}$$

Since the matrix is non-negative, it can be concluded that Equations (21) and (22) are the optimal solution of power distribution.

4.5. Finite State Machine Framework

In order to ensure that the proposed EMS can be adapt to different driving cycles and the fuel cell can work in the high efficient region, a finite state machine framework is built and five states are divided as follows:

State 0 : The hydrogen is exhausted (H_{2_remain} = 0) and the ultracapacitor SOC ≤ 10, or the vehicle stops for long time, $P_{uc} = 0$, $P_{fc} = 0$.

State 1 : The hydrogen is exhausted and the ultracapacitor SOC > 10, the ultracapacitor meet the power requirements of the vehicle for driving and braking, $P_{uc} = P_{dem}$, $P_{fc} = 0$.

State 2 : There is still a surplus of hydrogen (H_{2_remain}>0) and the ultracapacitor *SOC* > 90, the fuel cell turns off and the ultracapacitor work alone to supply energy to the vehicle for driving and braking, $P_{uc} = P_{dem}$, $P_{fc} = 0$.

State 3 : There is still a surplus of hydrogen and the ultracapacitor 90 ≥ SOC > 10, the fuel cell and the ultracapacitor work together to supply energy to the vehicle. The output power of the fuel cell and ultracapacitor is shown in Equations (21), (22). Note that while the vehicle is braking, the fuel cell continues to output energy to charge the ultracapacitor.

State 4 : There is still a surplus of hydrogen and the ultracapacitor 10 ≥ SOC, Part of the fuel cell output power meets the energy demand of motor, and the remaining part charges the ultracapacitor. $P_{fc} = P_{fcmax}$, $P_{uc} = P_{dem} - P_{fcmax}$.

The transition conditions between the states take into account the durability of the fuel cell and the *SOC* of ultracapacitor, the transition conditions are shown in Figure 4.

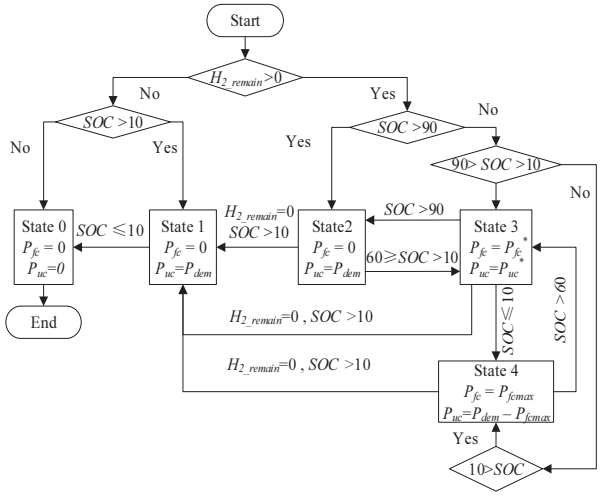

Figure 4. Finite state machine processes.

5. DETERMINATION OF WEIGHT COEFFICIENT

5.1. Weight Coefficient Design

When the ultracapacitor $SOC = SOC_{max} = 90$ or $SOC = SOC_{min} = 10$, $k_{sus} = 1$. When the ultracapacitor SOC is equal to the initial SOC_{ini}, $k_{sus} = 0$. Therefore, k_{sus} can be determined as:

$$k_{sus} = \left| 2\frac{SOC - SOC_{min}}{SOC_{max} - SOC_{min}} - 1 \right| \tag{24}$$

$$SOC_{ini} = \frac{SOC_{max} + SOC_{min}}{2} \tag{25}$$

k_{dua} and k_{eco} affect the durability and economy of fuel cell, and the relationship between weight coefficient is quantified by the allocation factor k in Equation (26). Once k is determined, the output power of fuel cell and ultracapacitor at every moment can be determined according to Equations (21) and (22). It should be noted that this algorithm is a real-time algorithm, which can adjust the output power of fuel cell and ultracapacitor in real time according to the current state and historical state, and obtain the optimal output power combination under the current state. In practical application, the allocation factor k can be obtained according to the actual vehicle calibration tests or expert experience. k_{dua}, k_{eco} satisfy the following formula:

$$\begin{cases} k_{dua} + k_{eco} = 1 - k_{sus} \\ k_{dua} = (1 - k_{sus})k \\ 1 \geq k \geq 0 \end{cases} \tag{26}$$

5.2. Optimization of Allocation Factor

In order to obtain the optimal k, an off-line simulation and optimization method is designed. which can help the real vehicle calibration. The methods are as follows:

1) Quantitative evaluation system: refer to Equations (4), (5) for fuel cell durability evaluation index. The economic evaluation index of the whole vehicle is quantified by the longest driving distance s. The initial operating condition of the vehicle is that the initial SOC of the ultracapacitor is 50 %, and the initial hydrogen mass is 1.2 kg. The stopping condition of the vehicle is that the remaining hydrogen mass is 0 kg, and the ultracapacitor $SOC \leq 50$ %.

2) Algorithm iteration: multi-objective optimization function is constructed as shown in Equation (27). The multi-objective artificial bee colony algorithm is applied with pareto solution set to obtain the optimal solution k. The specific process is shown in Table 1.

$$\min g(k) = \{-s, D_{fc}\} \tag{27}$$

Table 1. Algorithm process.

Process of multi-objective artificial bee colony algorithm
1. Initialize algorithm parameters such as optimization object k, number of iterations, bee population, etc.
2. Calculate the fitness values, and save historical ($-s_l$, $D_{fc,l}$).
3. Update k according to the artificial bee colony algorithm logic. Calculate the new fitness values, and save as ($-s$, D_{fc}).
4. **If** ($-s$, D_{fc}) dominates ($-s_l$, $D_{fc,l}$) according to Pareto solution set, ($-s_l = -s$, $D_{fc,l} = D_{fc}$) and go to step 3. **else**, go to step 5.
5. **If** the algorithm termination condition is reached, go to step 6. **else**, return to step 3.
6. Output the optimal k and end the optimization process.

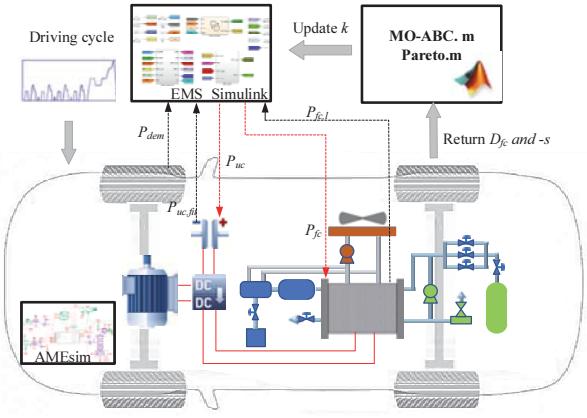

Figure 5. optimization flow and co-simulation.

3) The model in the loop (MIL) is realized based on SIMCENTER AMESIM(SIEMENS®) and MATLAB /Simulink (Mathworks®). The vehicle model is built in AMESim software and the EMS model is built in MATLAB/Simulink. In addition, multi-objective artificial bee colony algorithm and pareto set program are designed in MATLAB.m. The optimization flow and co-simulation with different software is shown in Figure 5.

6. RESULTS AND DISCUSSION

In this section, JC08, UDDS, NEDC and WLTP driving cycle are tested in simulation. The initial operating condition of the vehicle is that: the initial SOC of the ultracapacitor is 50 %, and the initial hydrogen mass is 1.2 kg. The stopping condition of the vehicle is that the remaining hydrogen mass is 0 kg, and the ultracapacitor SOC $\leq$ 50 %. After multi-objective optimization, the pareto

surface composed of mileage and fuel cell performance degradation under different driving cycles are shown in Figure 6. The allocation factor k under different driving cycles is sorted from small to large, as shown in Figure. 7. It can be seen from Figure. 8, the best allocation factor k is concentrated from 0.3 to 0.4. The partial optimal solutions on pareto surface and k under different driving cycles are shown in Table 2 ~ 5.

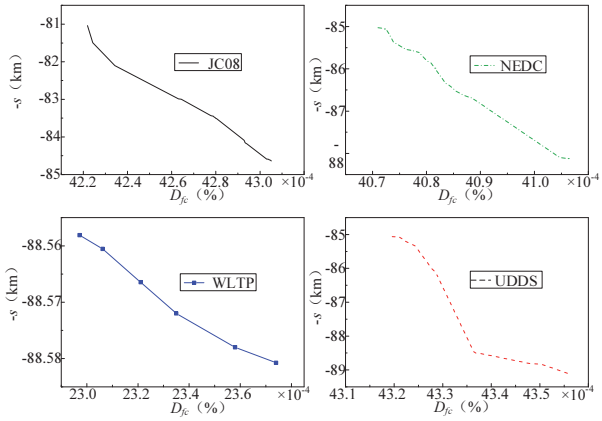

Figure 6. Pareto surface under different driving cycles.

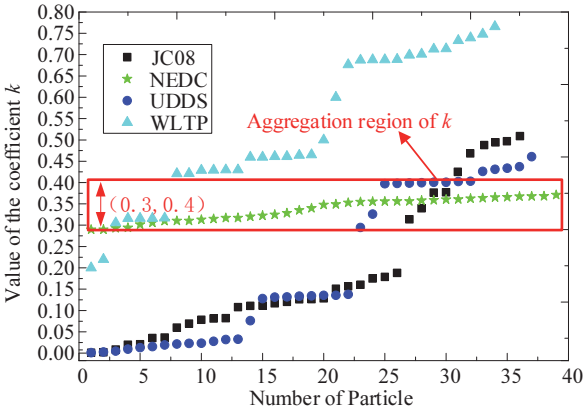

Figure 7. Allocation factor k under different driving cycles.

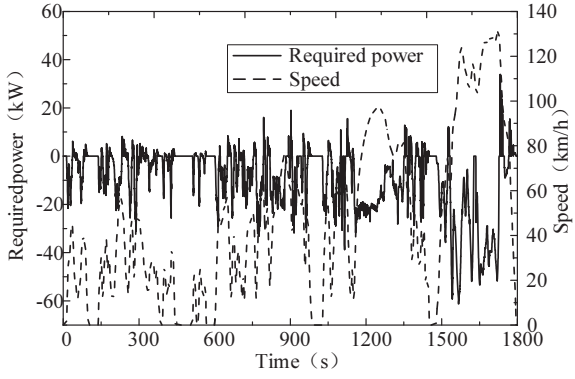

Figure 8. Required power and speed.

Table 2. Partial optimal solution under JC08.

Driving cycle	k	D_{fc} /($\times10^{-4}$%)	-s /(km)
JC08	0.02	42.64	-83.00
	0.11	42.92	-84.05
	0.15	43.03	-84.58
	0.16	43.04	-84.59
	0.34	42.24	-81.50
	…	…	…
	0.38	42.28	-81.04

Table 3. Partial optimal solution under NEDC.

Driving cycle	k	D_{fc} /($\times10^{-4}$%)	-s /(km)
NEDC	0.29	40.71	-85.03
	0.31	40.74	-85.39
	0.35	40.78	-85.59
	0.37	40.85	-86.53
	0.39	40.88	-86.66
	…	…	…
	0.42	41.07	-88.13

Table 4. Partial optimal solution under UDDS.

Driving cycle	k	D_{fc} /($\times10^{-4}$%)	-s /(km)
UDDS	0.01	43.21	-85.07
	0.02	43.21	-85.09
	0.13	43.28	-86.06
	0.14	43.29	-86.25
	0.43	43.37	-88.51
	…	…	…
	0.46	43.56	-89.11

Table 5. Partial optimal solution under WLTP.

Driving cycle	k	D_{fc} /($\times10^{-4}$%)	-s /(km)
WLTP	0.2	22.97	-88.53
	0.32	23.06	-88.54
	0.43	23.21	-88.55
	0.46	23.26	-88.56
	0.50	23.35	-88.57
	…	…	…
	0.69	23.74	-88.58

This paper shows the simulation results under WLTP and select $k = 0.35$.

Figure 9 shows the comparison of fuel cell output power curves under one WLTP driving cycle based on traditional power following strategy (PF) and optimal power following strategy (OP_PF). The output power of fuel cell based on PF strategy fluctuates greatly. Because its output power has a certain proportional relationship with ultracapacitor SOC and demand power. When the demand power is low, the output power of fuel cell based on PF is low, and the fuel cell runs under idling and high-power load conditions frequently. When the demand power is high, the output power of fuel cell is also high. When the demand power changes rapidly, the output power of fuel cell also changes synchronously and rapidly. In order to quickly recover the ultracapacitor SOC during braking state, the fuel cell continues to operate at the high efficiency point. When the current output power and historical output overpower cannot transition smoothly, the fuel cell power changes suddenly. Frequent power changes and idle operation accelerate the performance degradation of fuel cell. It can be seen that PF strategy accelerates the performance degradation of fuel cell when the load changes rapidly. The OP_ PF strategy can ensure the stability of fuel cell output power. When the demand power changes rapidly, the ultracapacitor responds to the rapidly changing demand power, and the fuel cell output power fluctuates in a small region.

Figure 10 shows the comparison of fuel cell efficiency curves under one WLTP driving cycle. Due to the large output power change of fuel cell with PF strategy, the efficiency of fuel cell with PF fluctuates greatly, and the efficiency of fuel cells is difficult to maintain near the high efficiency region. The output power of the fuel cell based on OP_PF strategy is stable and its fluctuation is small. Through reasonable algorithm design, the efficiency of the fuel cell can be maintained near the high efficiency region.

The fuel cell output power fluctuation with OP_PF strategy is small, and the power fluctuation of ultracapacitor is large. When the required power increases rapidly, the ultracapacitor provides the main part of the demand power. At this time, the *SOC* of the ultracapacitor changes greatly. The fuel cell output power fluctuation under PF strategy is large, the ultracapacitor power fluctuation is relatively small, and the change of ultracapacitor *SOC* is also small, PF strategy cannot give full play to the advantages of ultracapacitor. This phenomenon can also be seen from Figure 11.

In order to further compare the performance of the two control strategies under different single driving cycle, the two control strategies are compared from the aspects of equivalent hydrogen consumption and fuel cell performance degradation. The specific results are shown in Table 6. It can be concluded that compared with PF strategy, the equivalent hydrogen consumption and fuel cell performance degradation with OP_PF are both reduced under different single driving cycle.

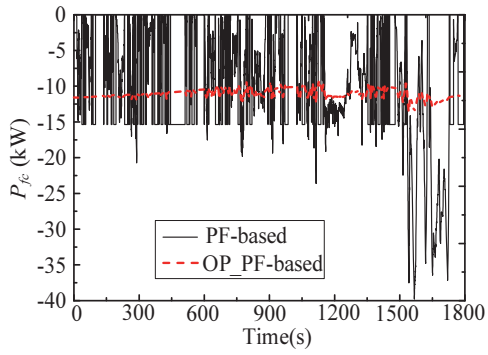

Figure 9. Comparison of fuel cell output power curves.

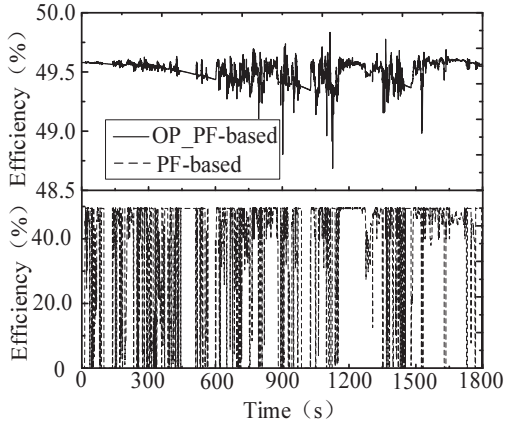

Figure 10. Comparison of fuel cell efficiency curves.

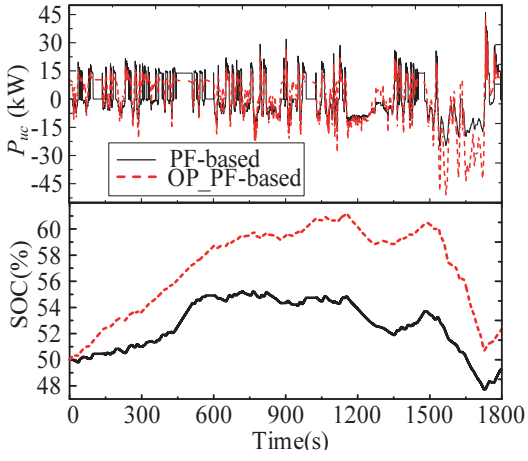

Figure 11. Comparison of the ultracapacitor output power and *SOC* curves.

Table 6. Comparison results of the two strategies under one driving cycle.

Single driving cycle	Strategy	Equivalent hydrogen consumption/(g)	D_{fc} /($\times 10^{-4}$ %)
JC08	PF-based	176.58	38.22
	OP_PF-bsaed	172.24	19.94
NEDC	PF-based	154.76	47.44
	OP_PF-bsaed	149.82	19.87
UDDS	PF-based	200.53	58.08
	OP_PF-bsaed	198.80	20.07
WLTP	PF-based	342.29	27.15
	OP_PF-bsaed	341.92	20.34

7. CONCLUSION

In this paper, an adaptive control strategy has been proposed for the EMS of fuel cell and ultracapacitor-based hybrid electric vehicles. Based on the traditional power following strategy, an optimal power following strategy is proposed. The proposed strategy takes into account the vehicle economy and component durability, the dynamic output characteristics of fuel cell are also satisfied. The optimization of energy distribution of fuel cell and ultracapacitor is realized. In order to balance economy and durability, MOABC algorithm is used to optimize the allocation factors within the strategy. The simulation results show that compared with the traditional power following strategy, the proposed energy management strategy can effectively extend the driving range, reduce the performance degradation of fuel cell. Compared with PF strategy, the equivalent hydrogen consumption of OP_PF is reduced by 0.37 g and the fuel cell degradation is reduced by 25.08 % under single WLTP driving cycle. The vehicle can travel 88.52 km with only 1.2 kg hydrogen consumption. The main contributions are as follows:

(1) The proposed control strategy can effectively reduce the power change of fuel cell, avoid the fuel cell running under idling and high-power load conditions. Once the fuel cell is started, it does not start and stop frequently, the performance degradation of fuel cell can be effectively reduced.
(2) The proposed control strategy can effectively make use of the characteristics of high power density of ultracapacitor, ensure the stable output power of fuel cell, control the output power of fuel cell to be stable in the high efficiency region, and effectively improve the economy of FCEV.
(3) The calculation process of the proposed control strategy is simple, the differential process only needs off-line derivation, and there is no complex on-line identification, learning and evolution process. It can be well applied to the actual vehicle, and the parameter optimization results can also provide a good reference value for the vehicle calibration.

ACKNOWLEDGEMENT–This work was supported by the Science and Technology Department of Jiangsu Province (Key Science and Technology Program of Jiangsu Province, BE2018 343-1); Senior Talent Fund through the Jiangsu University (20JDG 069); Jiangsu provincial colleges of Natural Science General Program (21KJB460028); China Postdoctoral Science Foundation (2021M 701477).

REFERENCES

Bin Wan Ramli, W. R., Pesyridis, A., Gohil, D. and Alshammari, F. (2020). Organic rankine cycle waste heat recovery for passenger hybrid electric vehicles. *Energies* **13**, **17**, 4532.

Bizon, N. and Thounthong, P. (2018). Fuel economy using the global optimization of the fuel cell hybrid power systems. *Energy Conversion and Management*, **173**, 665–678.

Borup, R. L., Kusoglu, A., Neyerlin, K. C., Mukundan, R., Ahluwalia, R. K., Cullen, D. A., More, K. L., Weber, A. Z. and Myers, D. J. (2020). Recent developments in catalyst-related PEM fuel cell durability. *Current Opinion in Electrochemistry*, **21**, 192–200.

Chen, C., Wang, J., Heo, Y. and Kishore, S. (2013). MPC-based appliance scheduling for residential building energy management controller. *IEEE Trans. Smart Grid* **4**, **3**, 1401–1410.

Chen, Z., Xiong, R., Wang, K. and Jiao, B. (2015). Optimal energy management strategy of a plug-in hybrid electric vehicle based on a particle swarm optimization algorithm. *Energies* **8**, **5**, 3661–3678.

Erdinc, O. and Uzunoglu, M. (2010). Recent trends in PEM fuel cell-powered hybrid systems: Investigation of application areas, design architectures and energy management approaches. *Renewable and Sustainable Energy Reviews* **14**, **9**, 2874–2884.

Fernández, R. Á., Caraballo, S. C., Cilleruelo, F. B. and Lozano, J. A. (2018). Fuel optimization strategy for hydrogen fuel cell range extender vehicles applying genetic algorithms. *Renewable and Sustainable Energy Reviews*, **81**, 655–668.

Geng, C., Jin, X. and Zhang, X. (2019). Simulation research on a novel control strategy for fuel cell extended-range vehicles. *Int. J. Hydrogen Energy* **44**, **1**, 408–420.

Gharibeh, H. F., Yazdankhah, A. S. and Azizian, M. R. (2020). Energy management of fuel cell electric vehicles based on working condition identification of energy storage systems, vehicle driving performance, and dynamic power factor. *J. Energy Storage*, **31**, 101760.

Hu, X., Han, J., Tang, X. and Lin, X. (2021). Powertrain design and control in electrified vehicles: A critical review. *IEEE Trans. Transportation Electrification* **7**, **3**,

1990–2009.

Hwang, J. J., Hu, J. S. and Lin, C. H. (2015). A novel range-extended strategy for fuel cell/battery electric vehicles. *The Scientific World J*., **2015**, 363094.

Karaoğlan, M. U., Kuralay, N. S. and Colpan, C. O. (2019). Investigation of the effects of battery types and power management algorithms on drive cycle simulation for a range-extended electric vehicle powertrain. *Int. J. Green Energy* **16**, **1**, 1–11.

Li, D., Xu, B., Tian, J. and Ma, Z. (2020). Energy management strategy for fuel cell and battery hybrid vehicle based on fuzzy logic. *Processes* **8**, **8**, 882.

Lian, R., Peng, J., Wu, Y., Tan, H. and Zhang, H. (2020). Rule-interposing deep reinforcement learning based energy management strategy for power-split hybrid electric vehicle. *Energy*, **197**, 117297.

Liu, Y., Liu, J., Zhang, Y., Wu, Y., Chen, Z. and Ye, M. (2020). Rule learning based energy management strategy of fuel cell hybrid vehicles considering multi-objective optimization. *Energy*, **207**, 118212.

Ma, L., Liu, N., Zhang, J., Tushar, W. and Yuen, C. (2016). Energy management for joint operation of CHP and PV prosumers inside a grid-connected microgrid: A game theoretic approach. *IEEE Trans. Industrial Informatics* **12**, **5**, 1930–1942.

Mbuwir, B. V., Vanmunster, L., Thoelen, K. and Deconinck, G. (2021). A hybrid policy gradient and rule-based control framework for electric vehicle charging. *Energy and AI*, **4**, 100059.

Mebarki, N., Rekioua, T., Mokrani, Z. and Rekioua, D. (2015). Supervisor control for stand-alone photovoltaic/hydrogen/battery bank system to supply energy to an electric vehicle. *Int. J. Hydrogen Energy* **40**, **39**, 13777–13788.

Ouddah, N., Adouane, L. and Abdrakhmanov, R. (2018). From offline to adaptive online energy management strategy of hybrid vehicle using pontryagin's minimum principle. *Int. J. Automotive Technology* **19**, **3**, 571–584.

Qi, X., Luo, Y., Wu, G., Boriboonsomsin, K. and Barth, M. (2019). Deep reinforcement learning enabled self-learning control for energy efficient driving. *Transportation Research Part C: Emerging Technologies*, **99**, 67–81.

Rajabzadeh, M., Bathaee, S. M. T. and Golkar, M. A. (2016). Dynamic modeling and nonlinear control of fuel cell vehicles with different hybrid power sources. *Int. J. Hydrogen Energy* **41**, **4**, 3185–3198.

Song, K., Chen, H., Wen, P., Zhang, T., Zhang, B. and Zhang, T. (2018). A comprehensive evaluation framework to evaluate energy management strategies of fuel cell electric vehicles. *Electrochimica Acta*, **292**, 960–973.

Sorlei, I. S., Bizon, N., Thounthong, P., Varlam, M., Carcadea, E., Culcer, M., Iliescu, M. and Raceanu, M. (2021). Fuel cell electric vehicles—A brief review of current topologies and energy management strategies. *Energies* **14**, **1**, 252.

Sulaiman, N., Hannan, M. A., Mohamed, A., Ker, P. J., Majlan, E. H. and Daud, W. W. (2018). Optimization of energy management system for fuel-cell hybrid electric vehicles: Issues and recommendations. *Applied Energy*, **228**, 2061–2079.

Sun, Z., Wang, Y., Chen, Z. and Li, X. (2020). Min-max game based energy management strategy for fuel cell/supercapacitor hybrid electric vehicles. *Applied Energy*, **267**, 115086.

Wang, Y., Sun, Z. and Chen, Z. (2019). Rule-based energy management strategy of a lithium-ion battery, supercapacitor and PEM fuel cell system. *Energy Procedia*, **158**, 2555–2560.

Xie, R., Ma, R., Pu, S., Xu, L., Zhao, D. and Huangfu, Y. (2020). Prognostic for fuel cell based on particle filter and recurrent neural network fusion structure. *Energy and AI*, **2**, 100017.

Yu, Y. X. and Ahn, K. K. (2019). Optimization of energy regeneration of hybrid hydraulic excavator boom system. *Energy Conversion and Management*, **183**, 26–34.

Zhang, H., Li, X., Liu, X. and Yan, J. (2019). Enhancing fuel cell durability for fuel cell plug-in hybrid electric vehicles through strategic power management. *Applied Energy*, **241**, 483–490.

Zhang, T., Wang, P., Chen, H. and Pei, P. (2018). A review of automotive proton exchange membrane fuel cell degradation under start-stop operating condition. *Applied Energy*, **223**, 249–262.

Zheng, C. H., Oh, C. E., Park, Y. I. and Cha, S. W. (2012). Fuel economy evaluation of fuel cell hybrid vehicles based on equivalent fuel consumption. *Int. J. Hydrogen Energy* **37**, **2**, 1790–1796.

Zhou, W., Yang, L., Cai, Y. and Ying, T. (2018). Dynamic programming for new energy vehicles based on their work modes Part II: Fuel cell electric vehicles. *J. Power Sources*, **407**, 92–104.

Zhou, Y., Li, H., Ravey, A. and Péra, M. C. (2020). An integrated predictive energy management for light-duty range-extended plug-in fuel cell electric vehicle. *J. Power Sources*, **451**, 227780.